Arabian Journal of Chemistry (2023) **16**, 104794

King Saud University

Arabian Journal of Chemistry

www.ksu.edu.sa
www.sciencedirect.com

ORIGINAL ARTICLE

Inhibition of $Fe_4Ge_3O_{12}$ formation in the leaching process of zinc oxide dust containing germanium by ultrasonic and iron powder

Ming Liang, Haokai Di, Yan Hong, Leiting Song, Jie Dai, Kun Yang [1], Libo Zhang [1]

State Key Laboratory of Complex Nonferrous Metal Resources Clean Utilization, Kunming University of Science and Technology, Kunming, Yunnan 650093, China
Yunnan Provincial Key Laboratory of Intensification Metallurgy, Kunming, Yunnan 650093, China
Faculty of Metallurgical and Energy Engineering, Kunming University of Science and Technology, Kunming, Yunnan 650093, China

Received 13 January 2023; accepted 6 March 2023
Available online 14 March 2023

KEYWORDS

Inhibition;
Reduction leaching;
Zinc oxide dust;
Germanium;
Ultrasonic;
Iron powder

Abstract Low leaching efficiency of germanium has always been a difficult point hindering the efficient utilization of zinc oxide dust containing germanium. Based on the previous research results that the formation of insoluble $Fe_4Ge_3O_{12}$ leads to germanium loss in the leaching process, a new process of reduction leaching of zinc oxide dust containing germanium enhanced by ultrasonic and iron powder is proposed. Under optimized conditions, the germanium leaching efficiency can be increased by 9.17%, reaching 93.43%. When leaching, the addition of iron powder can reduce the Fe^{3+} formed in the leaching process and hinder the formation of insoluble $Fe_4Ge_3O_{12}$, which can increase the leaching efficiency of germanium by 5.30%. At the same time, strong mechanical action of ultrasonic can fully disperse the iron powder in the leaching system, avoiding the phenomenon of insufficient local reduction. More importantly, the addition of ultrasonic can reduce the dissolved oxygen in the solution system and produce strong reducing hydrogen free radicals (·H), strengthening the reduction leaching effect, thus the germanium leaching efficiency is further increased by 3.87%. The research results provide a new method and theoretical guidance for the efficient utilization of zinc oxide dust containing germanium, which is of great significance.

1. Introduction

Germanium is a kind of rare and scattered metal, widely distributed in nature, such as copper ore, iron ore, sulfide ore and even rock, soil and spring water contain trace amounts of germanium. However, germanium is very dispersed, and there is almost no concentrated germanium ore. It is basically impossible to extract germanium in large quantities from certain ores, so the annual output of germanium is not high (Geng et al., 2022a, Kamran Haghighi and Irannajad 2022). Germa-

[1] Authors to.
E-mail addresses: truepsyche@sina.com (K. Yang), zhanglibopaper@126.com (L. Zhang)
Peer review under responsibility of King Saud University.

Production and hosting by Elsevier

https://doi.org/10.1016/j.arabjc.2023.104794
1878-5352

nium is usually extracted from intermediate products of nonferrous smelting process, lignite or secondary resources. As an important strategic resource and having many special properties, germanium plays an irreplaceable role in the national defense industry, aerospace, modern communication and other fields(Nusen et al., 2015, Libo Zhang 2016, Ruiz et al., 2018, Wang et al., 2020, Nguyen and Lee 2021, Tao et al., 2021, Geng et al., 2022b, Xi et al., 2022). It is of great significance to study and improve the efficient utilization of germanium resources.

Zinc oxide dust containing germanium is one of the essential raw materials for extracting germanium, which is obtained by fuming the intermediate product of lead–zinc smelting process. Generally, germanium extraction from zinc oxide dust containing germanium is treated by acid leaching process, dissolving valuable metal components such as zinc and germanium. And then zinc and germanium are refined into pure metal through a series of subsequent processes (Kamran Haghighi et al., 2018, Jiang et al., 2019, Jiang et al., 2020a). At the time of acid immersion, the leaching efficiency of the germanium was only about 70%, restricting the efficient utilization of zinc oxide dust. In order to solve the problem, scholars have carried out many studies (Liu et al., 2017, Song et al., 2021). Oxygen pressure acid leaching can make the leaching efficiency of germanium reach 89.72%. However, due to the high equipment cost and maintenance cost, this technology is difficult to be widely used (Liu et al., 2016, Wang et al., 2020, Xi et al., 2022, Li et al., 2023). Multistage extraction can enhance the leaching of germanium to a certain extent, but the process flow is long and the operation is complex, which causes a huge economic burden on the enterprise (Cheng et al., 2018). After microwave pretreatment, the leaching efficiency of germanium can be increased to 90%, but it is difficult to adapt to the current process, so it can't be industrialized (Wang et al., 2017a, Chen et al., 2018). Adding oxidants, such as O_2, H_2O_2, O_3, MnO_2, etc. to assist germanium leaching can release PbS and ZnS wrapped germanium to a certain extent, but there are also unavoidable problems: $Fe^{2+}$is oxidized to Fe^{3+}, which is easy to hydrolyze and adsorb germanium or react with germanium in solution, resulting in germanium re-entering the slag (Jiang et al., 2020b, Xin et al., 2021, Zhu et al., 2021, Xin et al., 2022). Current acid leaching technology still has industrial advantages. On this basis, it is of great economic and social significance to study how to improve the leaching efficiency of germanium economically and efficiently.

Ultrasonic has the characteristics of high frequency, high power, short wavelength, low diffraction and high energy (Monsef et al., 2018, Almessiere et al., 2019). It is widely used in industry, agriculture, military, medicine and other fields (Cintas et al., 2011, Cobley 2013). Because of its distinctive mechanical effect and cavitation effect, ultrasonic is often used as an external field strengthening means in metallurgical process (Wang et al., 2017b, Jiang et al., 2018, Yuan et al., 2018, Chen et al., 2021, Ding et al., 2022). When the ultrasonic wave propagates in liquid, the mechanical effect can strengthen the dispersion of fine particles or the mixing between solutions, thereby accelerating heat and mass transfer (Ghiyasiyan-Arani et al., 2017). The cavitation effect of ultrasonic can generate local high pressure and high temperature in liquid, which provides a new and very special environment for chemical reactions that are difficult or impossible to achieve under general conditions, and promotes or accelerates chemical reactions (Etschmann et al., 2017, Li et al., 2018). Therefore, utilization of ultrasonic to strengthen the leaching process is worth studying.

In previous studies, we found that during leaching, Fe (II) in the system was oxidized to Fe (III), and reacted with the leached germanium to form $Fe_4Ge_3O_{12}$ precipitation, resulting in the decline of germanium leaching efficiency (Liang et al., 2022). In this paper, based on the conventional acid leaching technology, iron powder and ultrasonic are added to strengthen reduction leaching, and then explain the mechanism of iron powder and ultrasound inhibiting the formation of $Fe_4Ge_3O_{12}$, aiming to improve the leaching efficiency of germanium and provide a new method and theoretical basis for the efficient leaching of zinc oxide dust containing germanium.

2. Experiments and characterization

2.1. Experiments

The sulfuric acid solution is used for leaching, and a certain amount of iron powder and specific power of ultrasonic are added during the leaching, so as to achieve the effect of ultrasonic assisted iron powder in strengthening the reduction leaching of zinc oxide dust containing germanium. After solid–liquid separation, the leaching solution and leaching residue are characterized to calculate the leaching efficiency of germanium and conduct theoretical analysis. The leaching equipment is illustrated in Fig. 1. The ultrasonic equipment used is an intelligent numerical control ultrasonic generator manufactured in Hangzhou, China, with the model of GBS-SCL 10A, frequency of 19838 Hz and power range of 0–1000 W. As can be viewed, in the thermostatic water bath, the ultrasonic probe is extended to the solution system for leaching experiment.

2.2. Characterization methods

RIGAKU TTR III X-ray diffractometer (XRD) (Cu target, Kα1, $\lambda = 0.15406$ nm) was used to determine the phase in the solid sample. Use PerkinElmer 8300 Coupled Plasma Optical Emission Spectrometry (ICP-OES) with detection limit of μg/L and error of less than 1.5% to detect the content of germanium. ICETM3500 Atomic Absorption Spectroscopy (AAS) with detection limit of $1 \times 10^{-8} \sim 1 \times 10^{-14}$ g and error range of 0.5% ~2.0% is used to determine the content of other key elements. The surface morphology and surface element composition of the samples were analyzed by scanning electron microscope (SEM) with XL30ESEM-TMP accelerating voltage of 15 kV. The JXA-8530F PLUS electron probe microanalyzer (EPMA) with detection limit of 0.01%~0.05% and relative error of less than 2% is used to plot the distribution of related elements in solid samples at 15 kV and 10nA. German Bruker A300 electron paramagnetic resonance (EPR) is used to capture the possible ·H produced during the reduction leaching process. Use JPSJ-605F dissolved oxygen tester to measure the content of dissolved oxygen in solution and its measuring range: 0–20.00 mg/L, the error is less than 0.1 mg/L. The above characterization is usually completed at the Analysis and Testing Center of Kunming University of Technology, Yunnan Nonferrous Metals and Products Quality Supervision and Inspection Station and Hangzhou Yanqu Information Technology Co., Ltd.

3. Results and discussion

3.1. Materials

Zinc oxide dust containing germanium used comes from the lead and zinc smelting industry. As showed in Table 1, it mainly contains zinc, lead, iron, sulfur, and germanium, with the contents of 51.13%, 14.41%, 3.06%, 3.57% and 657.87 g/t respectively, which has high recovery value.

XRD spectrum (Fig. 2) of zinc oxide dust containing germanium shows that its phases include ZnO, PbS, $PbSO_4$ and ZnS. In addition, its Electron Probe Micro Analysis (EPMA)

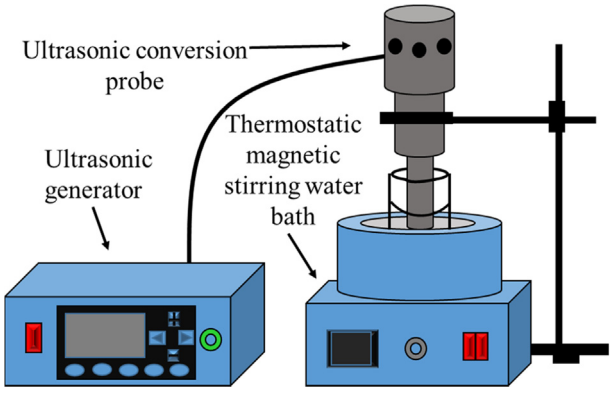

Fig. 1 Schematic diagram of zinc oxide dust containing germanium leaching equipment.

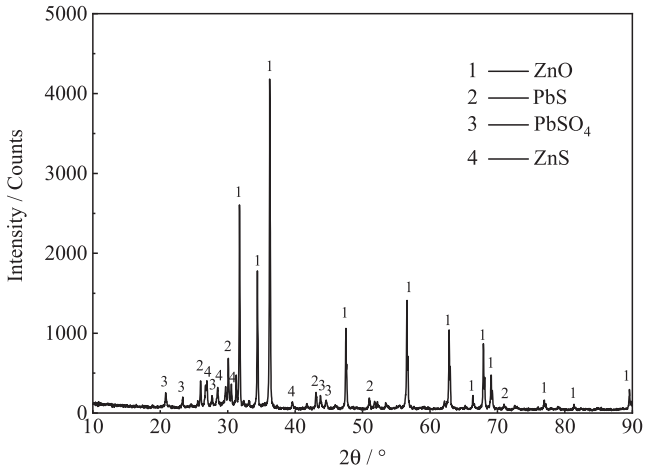

Fig. 2 XRD spectrum of zinc oxide dust containing germanium.

(Fig. 3) shows that the distribution of zinc and oxygen and sulfur, lead and oxygen and sulfur are relatively coincident, indicating that they combine with each other to form corresponding compounds, which is consistent with the results of XRD analysis. It is also worth noting that the distribution of germanium in the dust is relatively dispersed, and there is no obvious gathering area.

3.2. Optimization of leaching experiment

3.2.1. Reduction leaching of iron powder

In the previous study(Liang et al., 2022), the suitable experimental conditions for the leaching process were determined, namely, temperature 85° C, time 60 min, sulfuric acid concentration 150 g/L, liquid–solid ratio 5 mL:1 g. On this basis, relationship between amount of iron powder added and germanium leaching efficiency at different leaching time was studied. As shown in Fig. 4, when no iron powder is added, as previously studied, the leaching efficiency of germanium first increases, and then decreases after 30 min, up to 84.26% (Liang et al., 2022). After the addition of iron powder, the leaching efficiency of germanium gradually increases with time, and then tends to balance rather than decline. It is worth noting that germanium leaching efficiency increased with the increase of iron powder addition, and it will not continue to raise after the amount of iron powder is increased to 0.5% mass of the dust. After 50 min of leaching with 0.5% addition, the germanium leaching efficiency reached a balance of 89.56%, which was 5.30% higher than that without addition. Reduction leaching of zinc oxide dust containing germanium with iron powder has achieved good results. Table 2 shows the content of germanium in the leaching residue and the leaching efficiency of germanium in this experiment. When the germanium leaching efficiency reaches 89.56%, the germanium content in the slag decreases to 208.13 g/t, which is still relatively high.

At the same time, the content of Fe^{2+} and Fe^{3+} in the leaching process was detected, as shown in Fig. 5. When iron powder is not added, the content of both increases gradually before 30 min, and decreases to varying degrees after 30 min. After 30 min, the content of Fe^{3+} reached 0.247 g/L. After adding iron powder, the content of Fe^{3+} decreased significantly while the content of Fe^{2+} increased significantly. When the addition amount is increased to 0.5%, the content of Fe^{2+} and $Fe^{3+}$is maintained at a stable value of 3.235 g/L and 0.014 g/L respectively after 40 min of leaching.

3.2.2. Ultrasonic enhanced reduction leaching

Under the optimum condition that the iron powder content is 0.5% of the dust mass, ultrasonic was put in place to enhance the reduction leaching of germanium bearing zinc oxide soot. As showed in Fig. 6, after ultrasonic enhanced leaching, germanium leaching efficiency is significantly improved. Germanium leaching efficiency increases with the increase of ultrasonic power; after reaching 300 W, germanium leaching efficiency is basically unchanged. Under the condition of 300 W ultrasonic power, the germanium leaching efficiency is 93.43% when reaching equilibrium, which is 3.87% higher than that without ultrasonic power, and 9.17% higher than that without ultrasonic power and iron powder. Ultrasonic plays a very useful role in strengthening the reduction leaching of iron powder. Table 3 shows the content of germanium in the leaching residue and the leaching efficiency of germanium in this experiment. When the germanium leaching rate reaches 9, the germanium content in the slag is 4, which has decreased a lot.

Table 1 Main element content of raw material.

Element	Zn	Pb	Fe	S	Ge*
wt%	51.13	14.41	3.06	3.57	657.87

Note: the unit of Ge* content is g/t.

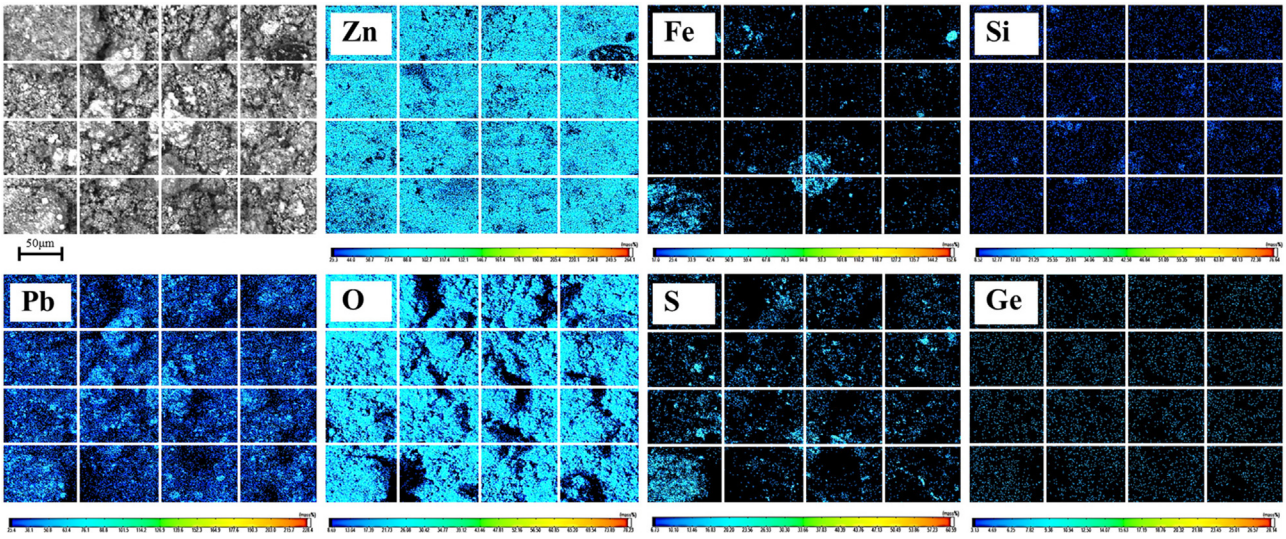

Fig. 3 EPMA of zinc oxide dust containing germanium.

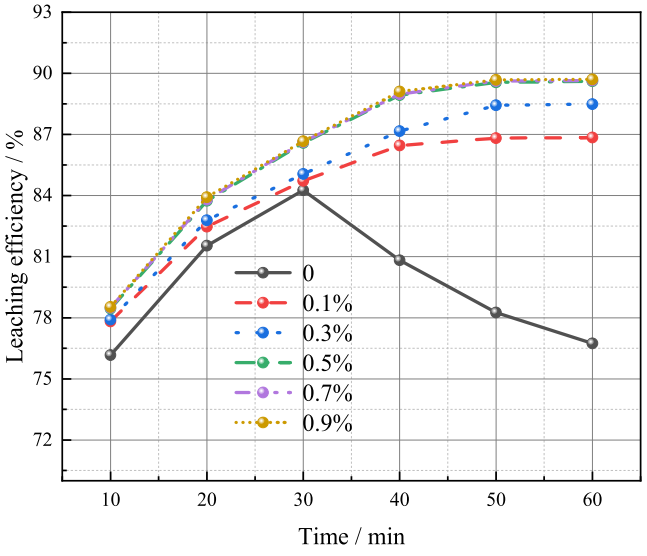

Fig. 4 Relationship between amount of the iron powder added and germanium leaching efficiency at different leaching time (sulfuric acid content: 150 g/L, temperature: 85 °C, liquid–solid ratio: 5:1).

3.3. Characterization of leaching residue

3.3.1. XRD characterization

From Fig. 7, we can note that after leaching, the main phases in the leached residue are $PbSO_4$, PbS and ZnS under any conditions. The ZnO phase is no longer detected, indicating that it has been basically leached. Before and after adding iron powder, the XRD pattern of slag has no obvious change, which suggests that iron powder has no effect on the leaching of zinc and lead. In addition, it is outstanding that the diffraction peak intensity of XRD of leaching residue under ultrasonic condition is weaker than that without ultrasonic condition. This is explained by the fact under ultrasonic condition, the leaching of zinc oxide dust containing germanium is more complete, which can also explain why the germanium leaching efficiency is further improved under ultrasonic condition.

3.3.2. EPMA characterization

In order to further confirm the leaching effect, the leached residue under ultrasonic condition was analyzed by EPMA. As showed in Fig. 8, the strength of Zn and O elements decreases significantly, indicating that ZnO is basically leached. Additionally, the distribution of Pb, O and S is basically the same, and also the distribution of Zn and S. Combined with the XRD analysis of leached slag in Section 3.2.1, the existence of $PbSO_4$, PbS and ZnS phases in the residue is further proved. It is worth noting that the distribution of Ge element is lower and more dispersed than that of the raw material, which is the result of the leaching of germanium in the raw material.

3.4. Mechanism of reduction leaching with iron powder

The potential-pH diagram of Ge-Fe-H_2O system at 25 ℃ is drawn according to relevant literature (Wang Jikun 2005, Lei Ting 2011) and FactSage database, which can directly understand the mutual equilibrium of various forms of compounds or ions in the reaction system under different redox potentials and pH values, as shown in Fig. 9. The relevant chemical reactions have been listed, see (1)–(21) for details.

$$H_2GeO_3 = HGeO_3^- + H^+ \quad (1)$$

$$HGeO_3^- = GeO_3^{2-} + H^+ \quad (2)$$

$$Ge^{2+} + 3H_2O = H_2GeO_3 + 4H^+ + 2e^- \quad (3)$$

$$Ge^{2+} + 3H_2O = HGeO_3^- + 5H^+ + 2e^- \quad (4)$$

$$Ge + H_2O = GeO + 2H^+ + 2e^- \quad (5)$$

$$GeO + H_2O = GeO_2 + 2H^+ + 2e^- \quad (6)$$

Table 2 Content of germanium in leaching slag and germanium leaching efficiency in the experiment of iron powder addition.

Addition	0		0.1%		0.3%		0.5%		0.7%		0.9%	
Time / min	Germanium content in slag / (g/t)	Germanium leaching efficiency / %	Germanium content in slag / (g/t)	Germanium leaching efficiency / %	Germanium content in slag / (g/t)	Germanium leaching efficiency / %	Germanium content in slag / (g/t)	Germanium leaching efficiency / %	Germanium content in slag / (g/t)	Germanium leaching efficiency / %	Germanium content in slag / (g/t)	Germanium leaching efficiency / %
10	475.06	76.17	442.17	77.82	440.37	77.91	429.61	78.45	428.81	78.49	428.01	78.53
20	368.01	81.54	349.47	82.47	343.09	82.79	324.15	83.74	322.95	83.8	320.56	83.92
30	313.78	84.26	304.61	84.72	297.84	85.06	267.53	86.58	266.54	86.63	265.74	86.67
40	382.36	80.82	269.93	86.46	255.97	87.16	220.69	88.93	219.69	88.98	217.10	89.11
50	433.40	78.26	262.75	86.82	230.65	88.43	208.13	89.56	206.93	89.62	205.73	89.68
60	463.70	76.74	262.15	86.85	229.46	88.49	207.13	89.61	206.33	89.65	205.14	89.71

$$GeO_2 + H_2O = HGeO_3^- + H^+ \quad (7)$$

$$GeO_2 + H_2O = GeO_3^{2-} + 2H^+ \quad (8)$$

$$Ge + 3H_2O = HGeO_3^- + 5H^+ + 4e^- \quad (9)$$

$$Ge + 3H_2O = GeO_3^{2-} + 6H^+ + 4e^- \quad (10)$$

$$GeO + 2H_2O = H_2GeO_3 + 2H^+ + 2e^- \quad (11)$$

$$GeO + 2H_2O = HGeO_3^- + 3H^+ + 2e^- \quad (12)$$

$$GeO + 2H_2O = GeO_3^{2-} + 4H^+ + 2e^- \quad (13)$$

$$GeH_4 = Ge + 4H^+ + 4e^- \quad (14)$$

$$Fe = Fe^{2+} + 2e^- \quad (15)$$

$$Fe^{2+} = Fe^{3+} + e^- \quad (16)$$

$$2Fe^{3+} + 3H_2O = Fe_2O_3 + 6H^+ \quad (17)$$

$$2Fe^{2+} + 3H_2O = Fe_2O_3 + 6H^+ + 2e^- \quad (18)$$

$$2Fe_3O_4 + H_2O = 3Fe_2O_3 + 2H^+ + 2e^- \quad (19)$$

$$3Fe(OH)_2 = Fe_3O_4 + 2H_2O + 2H^+ + 2e^- \quad (20)$$

$$Fe + 2H_2O = Fe(OH)_2 + 2H^+ + 2e^- \quad (21)$$

In the upper left corner area with low pH value and high oxygen potential, Fe^{3+} and H_2GeO_3 coexist, that is, the shaded area. Therefore, reducing the oxygen potential of the solution system during leaching can inhibit the production of Fe^{3+}, thus preventing Fe^{3+} reacts with H_2GeO_3 to form $Fe_4Ge_3O_{12}$ insoluble substances.

The Fe^{3+} content in the leaching process before and after the process optimization was detected. The content of Fe^{3+} in the leaching solution before the optimization was 247 mg/L, while the it was 14 mg/L after the optimization. After the optimization, the Fe^{3+} content declined significantly.

Leaching of zinc oxide dust containing germanium is a reaction process in contact with air. Therefore, when reduction leaching is not carried out, the Fe^{2+} ions in the system will be partially oxidized to Fe^{3+} (Formula (22)). Then Fe^{3+} will react with the leached germanium to form $Fe_4Ge_3O_{12}$ precipitation (Formula (23)), which makes germanium enter the slag, resulting in the decrease of germanium leaching efficiency. When adding iron powder for reductive leaching, the Fe^{3+} in the system (Formula (24)) can be reduced, and the iron ions in the system can be kept as Fe^{2+}, thus avoiding the loss of germanium caused by $Fe_4Ge_3O_{12}$ precipitation, and improving the germanium leaching efficiency. The Gibbs free energy of the relevant reaction at 348 K has been calculated according to the references (Yang 1983, Liang et al., 2022)

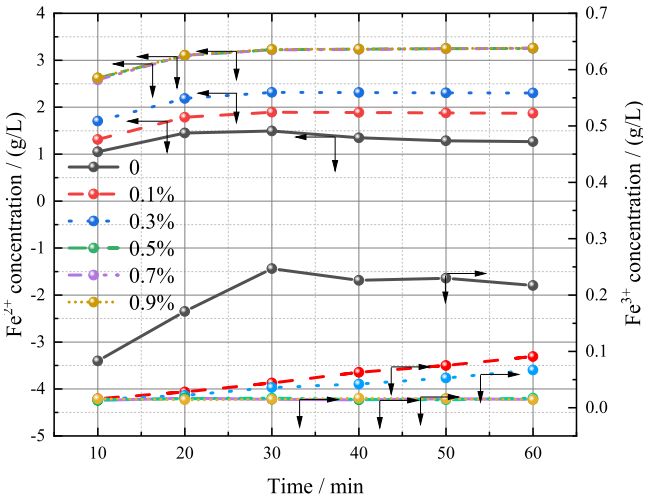

Fig. 5 Concentration of Fe^{2+} and Fe^{3+} at different leaching time (sulfuric acid content: 150 g/L, temperature: 85 °C, liquid–solid ratio: 5:1).

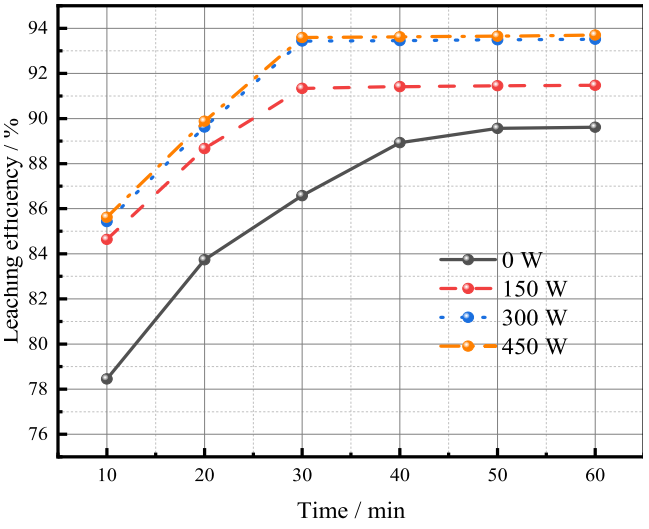

Fig. 6 Relationship between ultrasonic power and germanium leaching efficiency at different leaching time (sulfuric acid content: 150 g/L, temperature: 85 °C, liquid–solid ratio: 5:1, iron powder: 0.5% of dust mass).

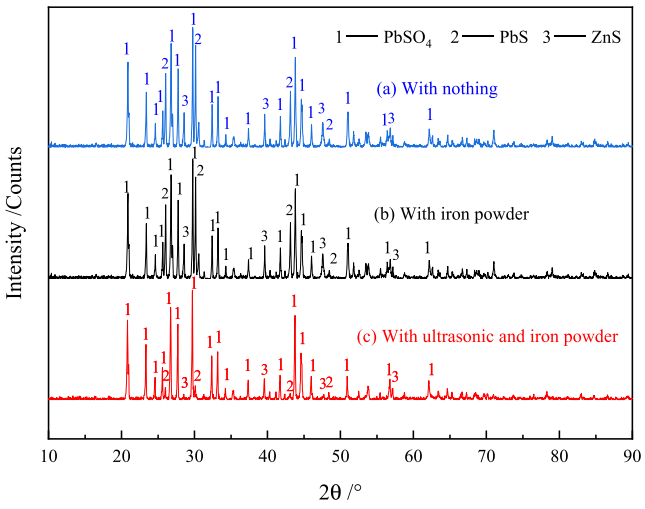

Fig. 7 XRD pattern of leaching residue ((a)With nothing, sulfuric acid content: 150 g/L, temperature: 85 °C, liquid–solid ratio: 5:1; (b) With iron power, sulfuric acid content: 150 g/L, temperature: 85 °C, liquid–solid ratio: 5:1, iron powder: 0.5% of dust mass; (b) With ultrasonic and iron power, ultrasonic power: 300 W, sulfuric acid content: 150 g/L, temperature: 85 °C, liquid–solid ratio: 5:1, iron powder: 0.5% of dust mass).

$$4Fe^{2+} + O_2 + 4H^+ = 4Fe^{3+} + 2H_2O \quad (22)$$

$$\begin{aligned}\Delta_r G^{\theta}_{348K}(22) &= 4\Delta_r G^{\theta}_{348K}(Fe^{3+}) \\ &+ 2\Delta_r G^{\theta}_{348K}(H_2O) - 4\Delta_r G^{\theta}_{348K}(Fe^{2+}) \\ &- \Delta_r G^{\theta}_{348K}(O_2) - 4\Delta_r G^{\theta}_{348K}(H^+) \\ &= -33.089\,kJ/mol\end{aligned}$$

$$4Fe^{3+} + 3H_2GeO_3 + 4H_2O = Fe_4Ge_3O_{12} + 12H^+ \quad (23)$$

$$\begin{aligned}\Delta_r G^{\theta}_{348K}(23) &= \Delta_r G^{\theta}_{348K}(Fe_2Ge_3O_{12}) + 12\Delta_r G^{\theta}_{348K}(H^+) \\ &- 3\Delta_r G^{\theta}_{348K}(H_2O) - 3\Delta_r G^{\theta}_{348K}(H_2GeO_4) \\ &- 4\Delta_r G^{\theta}_{348K}(Fe^{3+}) \\ &= -6.318\,kJ/mol\end{aligned}$$

$$Fe + 2Fe^{3+} = 3Fe^{2+} \quad (24)$$

Table 3 Content of germanium in leaching slag and germanium leaching efficiency in the experiment of ultrasonic power.

Power	0 W		150 W		300 W		450 W	
Time / min	Germanium content in slag / (g/t)	Germanium leaching efficiency / %	Germanium content in slag / (g/t)	Germanium leaching efficiency / %	Germanium content in slag / (g/t)	Germanium leaching efficiency / %	Germanium content in slag / (g/t)	Germanium leaching efficiency / %
10	429.61	78.45	306.21	84.64	290.46	85.43	286.67	85.62
20	324.15	83.74	225.87	88.67	206.93	89.62	201.75	89.88
30	267.53	86.58	172.84	91.33	130.98	93.43	127.79	93.59
40	220.69	88.93	171.25	91.41	130.58	93.45	127.19	93.62
50	208.13	89.56	170.45	91.45	129.78	93.49	126.59	93.65
60	207.13	89.61	170.05	91.47	129.38	93.51	125.59	93.7

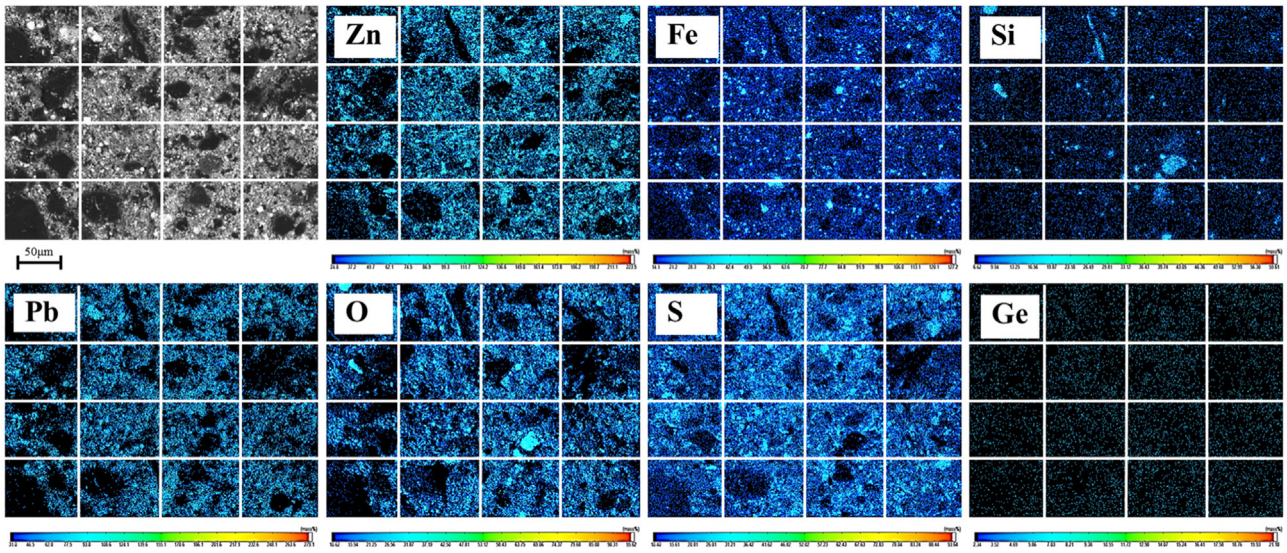

Fig. 8 EPMA elemental images of leaching residue (ultrasonic power: 300 W, sulfuric acid content: 150 g/L, temperature: 85 °C, liquid–solid ratio: 5:1, iron powder: 0.5% of dust mass).

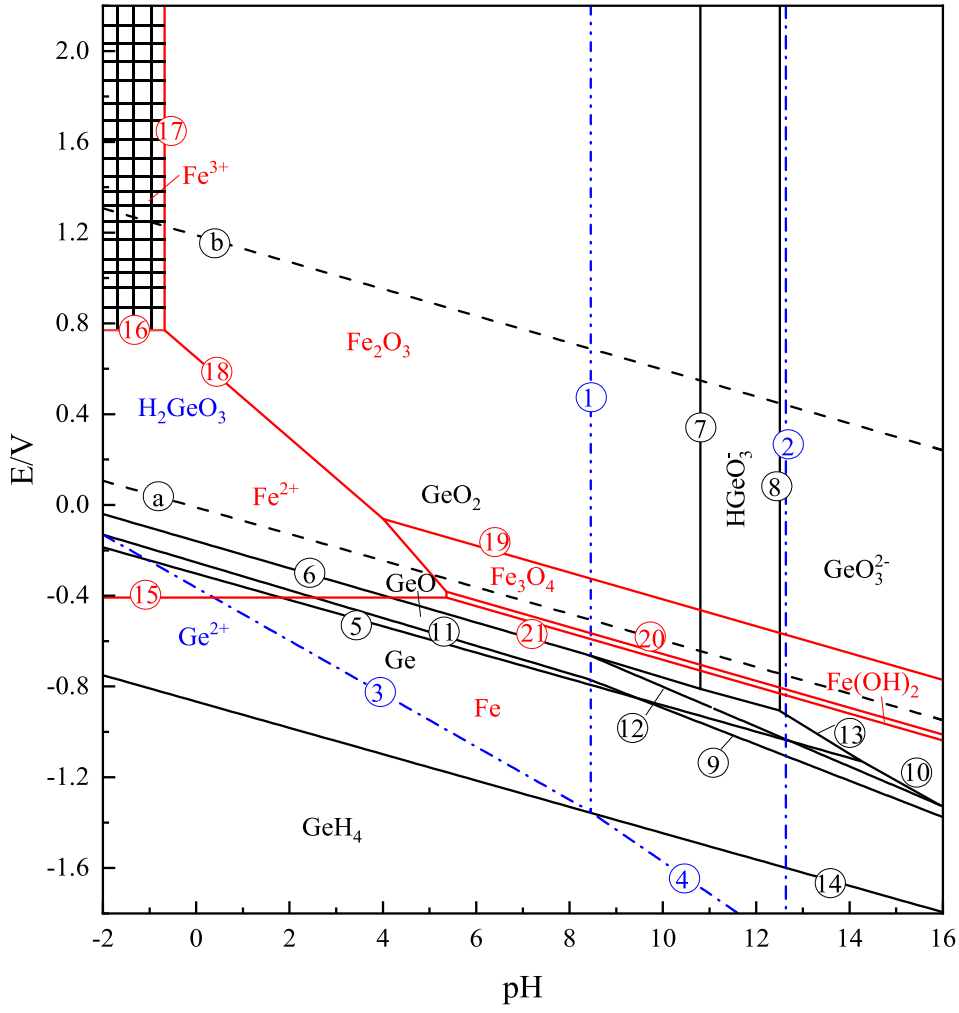

Fig. 9 Ge-Fe-H_2O potential-pH diagram at 25 ℃.

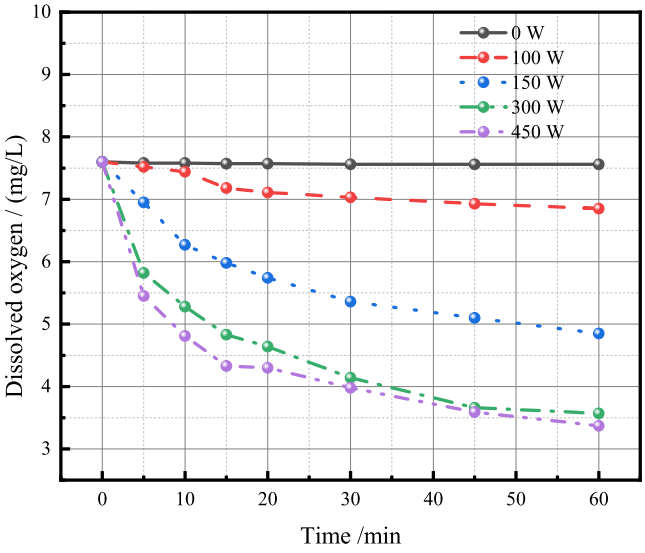

Fig. 10 Relationship between solution dissolved oxygen and ultrasonic action time under different ultrasonic power.

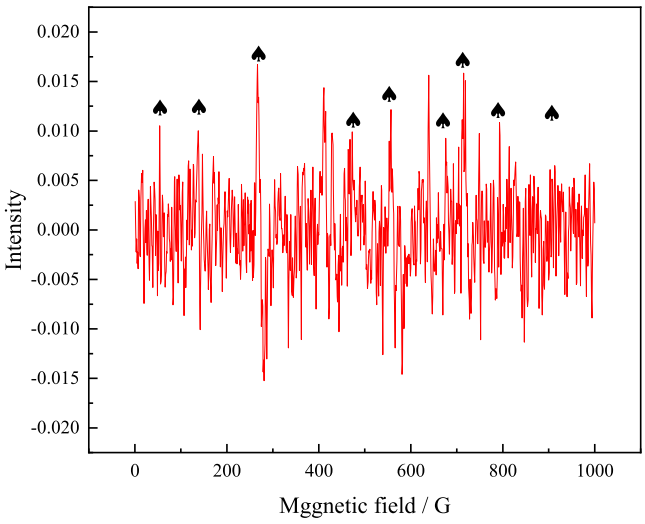

Fig. 11 EPR signal spectrum of DMPO·H in reductive leaching system of zinc oxide dust containing germanium enhanced by ultrasonic.

$$\begin{aligned}\Delta_r G^{\theta}_{348K}(24) &= 3\Delta_r G^{\theta}_{348K}\left(Fe^{2+}\right) - 2\Delta_r G^{\theta}_{348K}\left(Fe^{3+}\right) \\ &\quad - \Delta_r G^{\theta}_{348K}(Fe) \\ &= -56.677\,kJ/mol\end{aligned}$$

3.5. Mechanism of reduction leaching enhanced by ultrasonic

The strong mechanical action of ultrasonic can fully disperse the iron powder in the leaching system, avoiding the phenomenon of insufficient local reduction. In addition, ultrasonic can also strengthen the reduction leaching through the following two aspects.

3.5.1. Ultrasonic reduces dissolved oxygen

When ultrasonic acts on the solution system, the dissolved oxygen in the system can be decreased (Ozkan 2012, Gurpinar et al., 2013). As showed in Fig. 10, the higher the ultrasonic power, the lower the dissolved oxygen in the solution, and it basically tends to balance after 45 min. In addition, it is worth noting that 300 W ultrasonic power can reduce the dissolved oxygen content of the system at a lower level. After 30 min, the dissolved oxygen content is 45.24% lower than that without ultrasonic, reaching 4.14 mg/L. This is because the high temperature and high pressure environment caused by ultrasonic cavitation effect reduces the gas solubility of the solution system, and the oxygen in the solution escapes due to supersaturation. With the extension of ultrasonic action time, the oxygen in the solution reaches a new dissolution equilibrium. At this time, the dissolved oxygen in the solution is low, and oxygen no longer escapes. Hence, the decrease in dissolved oxygen in the solution can reduce the oxidation of Fe (Ⅱ) to a certain extent, so as to inhibit the formation of $Fe_4Ge_3O_{12}$ precipitation and avoid the decrease of the germanium leaching efficiency.

3.5.2. Generation of ·H by ultrasonic

Ultrasound can produce highly reducing ·H and highly oxidizing ·OH, and ·H is helpful to the reduction of Fe^{3+}. In order to explore the ultrasonic enhancement in the reduction leaching system of zinc oxide dust containing germanium, the generation of ·H captured by DMPO was detected by EPR and the results are as showed in Fig. 11. In this system, the peak height ratio of 1: 1:2:1:2:1:2:1:1, the nine fold characteristic peak signal DMPO·H (Yao et al., 2019, Zhou et al., 2019) shows that ultrasonic enhanced zinc oxide dust leaching system containing germanium can produce ·H, and because of the reductive environment created by iron powder, ·OH cannot be detected, so it is considered that only ·H is at work.

Strongly reductive ·H reacts with Fe (III) ions in the leaching system to change it into Fe (Ⅱ) ions, which inhibits the formation of $Fe_4Ge_3O_{12}$ precipitation, thus improving the germanium leaching efficiency.

$$H_2O \overset{\text{Ultrasonic}}{\Rightarrow} \cdot OH + \cdot H \tag{25}$$

4. Conclusions

In the process of leaching zinc oxide dust containing germanium, there is insoluble $Fe_4Ge_3O_{12}$ precipitate, which leads to germanium loss. Reducing leaching with iron powder can inhibit the formation of the $Fe_4Ge_3O_{12}$ precipitate; ultrasonic can enhance the effect of reducing leaching by strengthening mixing effect, reducing 45.24% dissolved oxygen in solution system and producing strong reducing hydrogen free radicals. After the new process of reduction leaching of zinc oxide dust containing germanium enhanced by 0.5% iron powder and 300 W ultrasonic power, the germanium leaching efficiency can be increased to 93.43%, which is of great significance for the efficient recovery of germanium and the utilization of Germanium-containing resources.

Declaration of Competing Interest

The authors declare that they have no known competing financial interests or personal relationships that could have appeared to influence the work reported in this paper.

Acknowledgement

This work was supported by the National Natural Science Foundation of China [grant number 51974141], Major Science and Technology Project of Yunnan Province [grant number 202202AB080005], the National Key Research and Development Program of China [grant number 2021YFC2902803] and Yunnan Fundamental Research Projects [grant number 202201BE070001-003].

References

Almessiere, M.A., Slimani, Y., Korkmaz, A.D., et al, 2019. Structural, optical and magnetic properties of Tm(3+) substituted cobalt spinel ferrites synthesized via sonochemical approach. Ultrason. Sonochem. 54, 1–10. https://doi.org/10.1016/j.ultsonch.2019.02.022.

Chen, B., Bao, S., Zhang, Y., 2021. Synergetic strengthening mechanism of ultrasound combined with calcium fluoride towards vanadium extraction from low-grade vanadium-bearing shale. Int. J. Min. Sci. Technol. 31, 1095–1106. https://doi.org/10.1016/j.ijmst.2021.07.008.

Chen, Y., Zhou, J., Zhang, L., et al, 2018. Microwave-assisted and regular leaching of germanium from the germanium-rich lignite ash. Green Process. Synth, 7, 538–545. https://doi.org/10.1515/gps-2017-0137.

Cheng, B., Zhang, K., Cao, Z., et al, 2018. Recovery of germanium from acid leach solutions of zinc refinery residue using an oxime extractant of HBL101. Metall. Res. Technol. 115, 510. https://doi.org/10.1051/metal/2018037.

Cintas, P., Palmisano, G., Cravotto, G., 2011. Power ultrasound in metal-assisted synthesis: From classical Barbier-like reactions to click chemistry. Ultrason Sonochem. 18, 836–841. https://doi.org/10.1016/j.ultsonch.2010.11.020.

Cobley, A., 2013. Ultrasound Sonochemistry – A more sustainable approach to surface modification? Surf. Eng. 25, 559–564. https://doi.org/10.1179/026708410x12459349720259.

Ding, W., Bao, S., Zhang, Y., et al, 2022. Mechanism and kinetics study on ultrasound assisted leaching of gallium and zinc from corundum flue dust. Miner. Eng. 183,. https://doi.org/10.1016/j.mineng.2022.107624 107624.

Etschmann, B., Liu, W., Li, K., et al, 2017. Enrichment of germanium and associated arsenic and tungsten in coal and roll-front uranium deposits. Chem. Geol. 463, 29–49. https://doi.org/10.1016/j.chemgeo.2017.05.006.

Geng, X., Liu, Y., Zhang, W., et al, 2022a. Recent advances in the recovery of germanium during the zinc refining process. Chem. Eng. J. 446,. https://doi.org/10.1016/j.cej.2022.137445 137445.

Geng, X., Liu, Y., Zhang, W., et al, 2022b. Recent advances in the recovery of germanium during the zinc refining process. Chem. Eng. J. 137445. https://doi.org/10.1016/j.cej.2022.137445.

Ghiyasiyan-Arani, M., Salavati-Niasari, M., Naseh, S., 2017. Enhanced photodegradation of dye in waste water using iron vanadate nanocomposite; ultrasound-assisted preparation and characterization. Ultrason Sonochem. 39, 494–503. https://doi.org/10.1016/j.ultsonch.2017.05.025.

Gurpinar, G., Sonmez, E., Bozkurt, V., 2013. Effect of ultrasonic treatment on flotation of calcite, barite and quartz. Mineral Process. Extractive Metal. 113, 91–95. https://doi.org/10.1179/037195504225005796.

Jiang, F., Chen, Y., Ju, S., et al, 2018. Ultrasound-assisted leaching of cobalt and lithium from spent lithium-ion batteries. Ultrason Sonochem. 48, 88–95. https://doi.org/10.1016/j.ultsonch.2018.05.019.

Jiang, T., Zhang, T., Ye, F., et al, 2019. Occurrence state and sulfuric-acid leaching behavior of germanium in secondary zinc oxide. Miner. Eng. 137, 334–343. https://doi.org/10.1016/j.mineng.2019.04.020.

Jiang, T., Zhang, T., Liu, Z., 2020a. Recovery of Germanium via H_2SO_4/MnO_2 Leaching–NaAc leaching/Na_2CO_3 precipitation–tri (octyl-decyl) amine stepwise solvent extraction. ACS Sustain. Chem. Eng. 8, 18545–18557. https://doi.org/10.1021/acssuschemeng.0c06526.

Jiang, T., Zhang, T., Liu, Z., 2020b. Recovery of Germanium via H_2SO_4/MnO_2 Leaching–NaAc Leaching/Na_2CO_3 Precipitation–Tri(octyl-decyl) Amine Stepwise Solvent Extraction. ACS Sustain. Chem. Eng. 8, 18545–18557. https://doi.org/10.1021/acssuschemeng.0c06526.

Kamran Haghighi, H., Irannajad, M., 2022. Roadmap for recycling of germanium from various resources: reviews on recent developments and feasibility views. Environ. Sci. Pollut. Res. 29, 48126–48151. https://doi.org/10.1007/s11356-022-20649-5.

Kamran Haghighi, H., Irannajad, M., Fortuny, A., et al, 2018. Recovery of germanium from leach solutions of fly ash using solvent extraction with various extractants. Hydrometall. 175, 164–169. https://doi.org/10.1016/j.hydromet.2017.11.006.

Lei Ting, W.S., Yanmei, Z., 2011. Germanium metallurgy. Metallurgical industry press, Beijing.

Li, Y., He, X., Yang, Y., et al, 2023. High pressure acid leaching of low germanium bearing silica residue (GRS): Characterization of leach residue and mechanistic details of germanium leaching. Hydrometall. 216,. https://doi.org/10.1016/j.hydromet.2022.106015 106015.

Li, H., Li, S., Srinivasakannan, C., et al, 2018. Efficient cleaning extraction of silver from spent symbiosis lead-zinc mine assisted by ultrasound in sodium thiosulfate system. Ultrason Sonochem. 49, 118–127. https://doi.org/10.1016/j.ultsonch.2018.07.034.

Liang, M., Di, H., Song, L., et al, 2022. Study on leaching behaviour of germanium and iron in zinc oxide dust from lead zinc smelting. Can. Metall. Q. 1–8. https://doi.org/10.1080/00084433.2022.2114126.

Libo Zhang, W.G., Peng, J., Li, J., Lin, G., Xia, Y.u., 2016. Comparison of ultrasonic-assisted and regular leaching of germanium from by-product of zinc metallurgy. Ultrason Sonochem. 31, 143–149. https://doi.org/10.1016/j.ultsonch.2015.12.006.

Liu, F., Liu, Z., Li, Y., et al, 2016. Extraction of gallium and germanium from zinc refinery residues by pressure acid leaching. Hydrometall. 164, 313–320. https://doi.org/10.1016/j.hydromet.2016.06.006.

Liu, F., Liu, Z., Li, Y., et al, 2017. Recovery and separation of gallium (III) and germanium(IV) from zinc refinery residues : Part II: Solvent extraction. Hydrometall. 171, 149–156. https://doi.org/10.1016/j.hydromet.2017.05.009.

Monsef, R., Ghiyasiyan-Arani, M., Salavati-Niasari, M., 2018. Application of ultrasound-aided method for the synthesis of $NdVO_4$ nano-photocatalyst and investigation of eliminate dye in contaminant water. Ultrason Sonochem. 42, 201–211. https://doi.org/10.1016/j.ultsonch.2017.11.025.

Nguyen, T.H., Lee, M.S., 2021. A review on germanium resources and its extraction by hydrometallurgical method. Miner. Process. Extr. Metall. Rev. 42, 406–426. https://doi.org/10.1080/08827508.2020.1756795.

Nusen, S., Zhu, Z., Chairuangsri, T., et al, 2015. Recovery of germanium from synthetic leach solution of zinc refinery residues by synergistic solvent extraction using LIX 63 and Ionquest 801. Hydrometall. 151, 122–132. https://doi.org/10.1016/j.hydromet.2014.11.016.

Ozkan, S.G., 2012. Effects of simultaneous ultrasonic treatment on flotation of hard coal slimes. Fuel 93, 576–580. https://doi.org/10.1016/j.fuel.2011.10.032.

Ruiz, A.G., Sola, P.C., Palmerola, N.M., 2018. Germanium: current and novel recovery processes. Adv. Mater. Device Applications Germanium.

Song, J., Peng, C., Liang, Y., et al, 2021. Efficient extracting germanium and gallium from zinc residue by sulfuric and tartaric

complex acid. Hydrometall. 202. https://doi.org/10.1016/j.hydromet.2021.105599.

Tao, J., Tao, Z., Zhihong, L., 2021. Review on resources and recycling of germanium, with special focus on characteristics, mechanism and challenges of solvent extraction. J. Clean. Prod. 294,. https://doi.org/10.1016/j.jclepro.2021.126217 126217.

Wang, S., Cui, W., Zhang, G., et al, 2017a. Ultra fast ultrasound-assisted decopperization from copper anode slime. Ultrason Sonochem. 36, 20–26. https://doi.org/10.1016/j.ultsonch.2016.11.013.

Wang Jikun, H.A., 2005. Modern germanium metallurgy. Metallurgical industry press, Beijing.

Wang, W., Wang, F., Lu, F., 2017b. Microwave alkaline roasting-water dissolving process for germanium extraction from zinc oxide dust and its analysis by response surface methodology (RSM). Metall. Res. Technol. 115. https://doi.org/10.1051/metal/2017093.

Wang, Y., Wang, H., Li, X., et al, 2020. Study on the improvement of the zinc pressure leaching process. Hydrometall. 195. https://doi.org/10.1016/j.hydromet.2020.105400.

Xi, J., Ji, G., Liao, Y., et al, 2022. Research on separation and extraction of valuable metals from complex non-ferrous metals resources by high pressure oxygen leaching methodology: a review. J. Sustainable Metal. 8, 51–63. https://doi.org/10.1007/s40831-022-00502-2.

Xin, C., Xia, H., Zhang, Q., et al, 2021. Leaching of zinc and germanium from zinc oxide dust in sulfuric acid-ozone media. Arab. J. Chem. 14,. https://doi.org/10.1016/j.arabjc.2021.103450 103450.

Xin, C., Xia, H., Jiang, G., et al, 2022. Mechanism and kinetics study on ultrasonic combined with oxygen enhanced leaching of zinc and germanium from germanium-containing slag dust. Sep. Purif. Technol. 302,. https://doi.org/10.1016/j.seppur.2022.122167 122167.

Yang, X., 1983. Handbook of thermodynamic data calculation of high temperature aqueous solutions. Metallurgical Industry Press.

Yao, Q., Zhou, X., Xiao, S., et al, 2019. Amorphous nickel phosphide as a noble metal-free cathode for electrochemical dechlorination. Water Res. 165,. https://doi.org/10.1016/j.watres.2019.114930 114930.

Yuan, J., Xiao, J., Li, F., et al, 2018. Co-treatment of spent cathode carbon in caustic and acid leaching process under ultrasonic assisted for preparation of SiC. Ultrason Sonochem. 41, 608–618. https://doi.org/10.1016/j.ultsonch.2017.10.027.

Zhou, J., Lou, Z., Xu, J., et al, 2019. Enhanced electrocatalytic dechlorination by dispersed and moveable activated carbon supported palladium catalyst. Chem. Eng. J. 358, 1176–1185. https://doi.org/10.1016/j.cej.2018.10.098.

Zhu, Y., Deng, Z., Wei, C., et al, 2021. Adaptive process for improving leaching efficiency of germanium from secondary zinc oxide. Int. J. Chem. React. Eng. 19, 615–623. https://doi.org/10.1515/ijcre-2021-0012.